

On Electron Heating, Deposition Rate, and Ion Recycling in the High Power Impulse Magnetron Sputtering Discharge

Jón Tómas Guðmundsson^{1,2}

¹Space and Plasma Physics, KTH Royal Institute of Technology,
Stockholm, Sweden

² Science Institute, University of Iceland, Reykjavik, Iceland

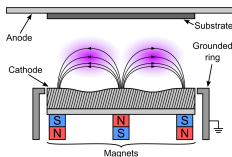
Sputtering & Plasma Process Group
Japan Society of Vacuum and Surface Science
September 2., 2021



Introduction – Magnetron sputtering

- Magnetron sputtering is a highly successful and widely used technique for thin film deposition

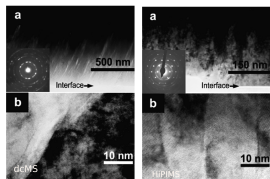
Gudmundsson (2020) PSST **29** 113001



Gudmundsson and Lundin (2020) in High Power Impulse Magnetron Sputtering Discharge, Elsevier, 2020

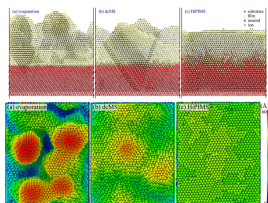
- Three fundamental topics will be discussed:
 - **Electron power absorption**
 - **Deposition rate**
 - **Recycling**

Introduction



Alami et al. (2005) JVSTA 23 278

- High power impulse magnetron sputtering (HiPIMS) provides higher ionized flux fraction than dc magnetron sputtering (dcMS)
- Due to the higher fraction of ionization of the sputtered species
 - the films are smooth and dense
 - control over phase composition and microstructure is possible
 - enhanced mechanical, electrical and optical properties
 - improved film adhesion

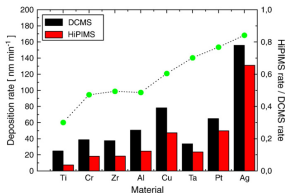


Kateb et al. (2019) JVSTA 37 031306



Introduction – Deposition rate

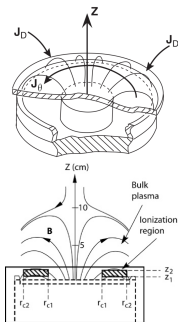
- There is a drawback
- The deposition rate is lower for HiPIMS when compared to dcMS operated at the same average power
- The HiPIMS deposition rates are typically in the range of 30 – 85% of the dcMS rates depending on target material
- Many of the ions of the target material are attracted back to the target surface by the cathode potential



From Samuelsson et al. (2010) SCT **202** 591

Ionization region model of HiPIMS

- The ionization region model (IRM) is a time-dependent volume averaged plasma chemical model of the ionization region (IR) of the HiPIMS discharge
- It gives the temporal evolution of the densities of ions, neutrals and electrons
- The IR is defined as an annular cylinder with outer radii r_{c2} , inner radii r_{c1} and length $L = z_2 - z_1$, extends from z_1 to z_2 axially away from the target



The definition of the volume covered by the IRM

From Raadu et al. (2011) PSST 20 065007

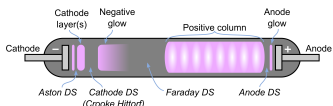
Detailed model description is given in

Huo et al. (2017) JPD 50 354008

Electron power absorption



Electron power absorption



T. J. Petty, LPGP, Université Paris Sud

Gudmundsson and Hecimovic (2017) PSST 26 123001

- A dc discharge with a cold cathode is sustained by secondary electron emission from the cathode due to ion bombardment
- The discharge current at the target consists of electron current I_e and ion current I_i or

$$I_D = I_e + I_i = I_i(1 + \gamma_{see})$$

where γ_{see} is the secondary electron emission coefficient

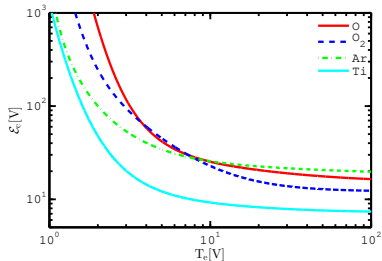
- Note that $\gamma_{see} \sim 0.05 - 0.2$ for most metals, so at the target ion current dominates

Electron power absorption

- These secondary electrons are accelerated in the cathode dark space
- They must produce sufficient number of ions to release more electrons from the cathode
- The number of electron-ion pairs created by each secondary electron is then

$$\mathcal{N} \approx \frac{V_D}{\mathcal{E}_c}$$

where \mathcal{E}_c is the energy loss per electron-ion pair created



Gudmundsson et al. (2016) PSST **25** 065004



Electron power absorption

- In magnetron sputtering effective secondary electron emission coefficient

$$\gamma_{\text{see,eff}} = m\epsilon_e(1 - r)\gamma_{\text{see}}$$

where r is the recapture probability

- To sustain the discharge the condition

$$\gamma_{\text{see,eff}}\mathcal{N} = 1$$

defines the minimum voltage

$$V_{D,\text{min}} = \frac{\mathcal{E}_c}{\beta\gamma_{\text{see,eff}}}$$

referred to as Thornton equation

Magnetron sputtering: basic physics and application to cylindrical magnetrons

John A. Thornton

July Corporation, 1811 Colorado Avenue, Santa Monica, California 90404

(Received 22 September 1977; accepted 7 December 1977)

Magnetron sputtering sources can be defined as diode devices in which magnetic fields are used in concert with the cathode surface to form electron traps which are so configured that the $E \times B$ electron-drift currents close on themselves. Cylindrical magnetron sputtering sources in which point or hollow cathodes are operated in axial magnetic fields have been reported for a number of years. However, their performance is limited by end losses. A remarkable performance is achieved when the end losses are eliminated by proper shaping of the magnetic field or by using suitably placed electron-reflecting surfaces. High currents and sputtering rates can be obtained, nearly independent of voltage, even at low pressures. This characteristic what has been defined as the magnetron mode of operation. This paper reviews the basic principles that underlie the operation of dc sputtering sources in the magnetron mode with particular emphasis on cylindrical magnetrons. The important attributes of these devices as sputtering sources are also reviewed.

PACS numbers: 81.15.-e, 52.75.-d

Thornton (1978) JVST **15**(2) 171

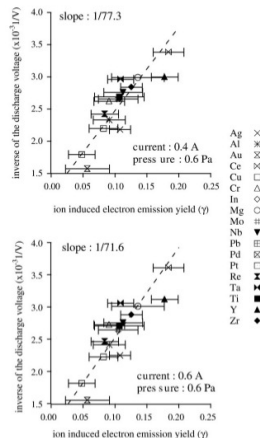


Electron power absorption

- We can rewrite the Thornton equation

$$\frac{1}{V_D} = \frac{\beta m \epsilon_e (1 - r)}{\mathcal{E}_c} \gamma_{\text{see}}$$

- A plot of the inverse discharge voltage $1/V_D$ against γ_{see} should then give a straight line through the origin
- Depla et al. measured the discharge voltage for 18 different target materials
- It can be seen that a straight line indeed results, but that it does not pass through the origin



Electron power absorption

- We have proposed that the intercept is due to Ohmic heating
- We can now write the inverse discharge voltage $1/V_D$ in the form of a generalized Thornton equation

$$\frac{1}{V_D} = \underbrace{\frac{\beta \epsilon_e^H m (1-r)(1-\delta_{IR})}{\mathcal{E}_C^H}}_a \gamma_{see} + \underbrace{\frac{\epsilon_e^C \langle I_e/I_D \rangle_{IR} \delta_{IR}}{\mathcal{E}_C^C}}_b$$

or

$$\frac{1}{V_D} = a \gamma_{see} + b$$

- We associate a with hot electrons e^H , sheath acceleration
- We associate b with the Ohmic heating process and cold electrons e^C



Electron power absorption

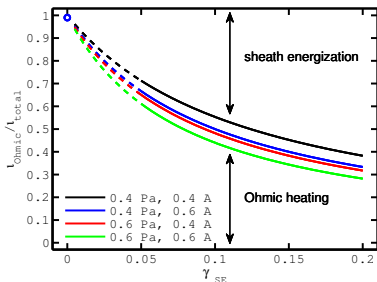
- The fraction of the total ionization that is due to Ohmic heating can be obtained directly from the line fit parameters a and b or as a function of only the secondary electron yield

 γ_{SE}

$$\frac{\iota_{Ohmic}}{\iota_{total}} = \frac{b}{a\gamma_{SE} + b}$$

- The fraction of the discharge voltage that falls over the ionization region

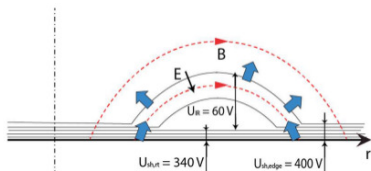
$$\delta_{IR} = \frac{V_{IR}}{V_D} = 0.15 - 0.19$$



From Brenning et al. (2016) PSST 25 061024

Electron power absorption

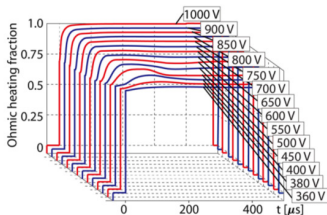
- The presence of a transverse magnetic field enables a potential drop to exist outside the cathode sheath
- A potential V_{SH} falls over the sheath, and the rest of the applied voltage, $V_{IR} = V_D - V_{SH}$, falls across the extended pre-sheath, the ionization region (IR), $\delta_{IR} = V_{IR}/V_D$
- Ohmic heating, the dissipation of locally deposited electric energy $\mathbf{J}_e \cdot \mathbf{E}$ to the electrons in the plasma volume outside the sheath



From Brenning et al. (2016) PSST **25** 065024

Electron power absorption

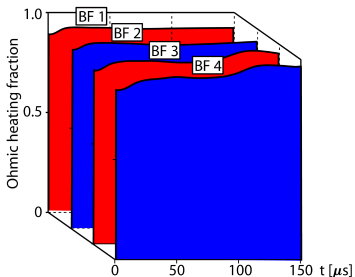
- Applying the ionization region model (IRM) to a HiPIMS discharge
- For the Al target, Ohmic heating is in the range of 87 % (360 V) to 99 % (1000 V)
- The domination of Al^+ -ions, which have zero secondary electron emission yield, has the consequence that there is negligible sheath energization
- The ionization threshold for twice ionized Al^{2+} , 18.8 eV, is so high that few such ions are produced



From Huo et al. (2017) JPD **50** 354003

Electron power absorption

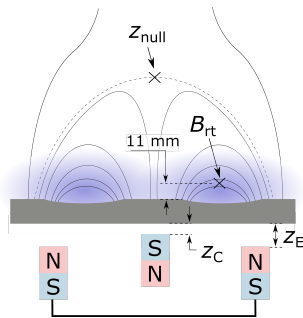
- For a Ti target Ohmic heating is about 92 %
 - Both Ar^+ and Ti^{2+} -ions contribute to creation of secondary electrons
- For Ti target in Ar/O_2 mixture
 - In the metal mode Ohmic heating is found to be 90 % during the plateau phase of the discharge pulse
 - For the poisoned mode Ohmic heating is 70 % with a decreasing trend, at the end of the pulse



From Huo et al. (2017) JPD **50** 354003

Electron power absorption

- There are indications that the ratio of Ohmic heating to sheath heating changes depending on the magnetic field configuration
- Magnetron assembly with definitions of the parameters B_{rt} and z_{null} , and the distance coordinates z_C and z_E for the central (C) and the annular edge (E) magnet with respect to their closest position to the rear of the target



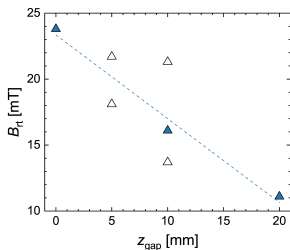
From Rudolph et al. (2021) JPD submitted for publication

Electron power absorption

- To describe the magnetic field we use a constructed parameter $z_{\text{gap}} = z_{\text{C}} + z_{\text{E}}$ instead of the 'classical' magnetic field parameters B_{rt} and z_{null}
- We analyze discharges with Ti target with adjustable confining magnetic field

Hajihoseini et al. (2019) Plasma 2 201

- The total power that is necessary to heat electrons by Ohmic heating is only 10 – 20 % compared to the power needed to heating electrons by the same amount in the sheath

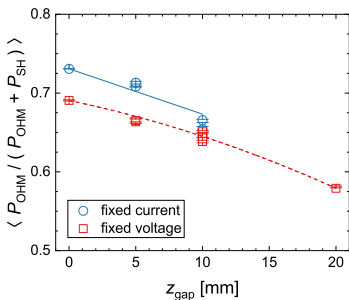


From Rudolph et al. (2021) JPD submitted for publication



Electron power absorption

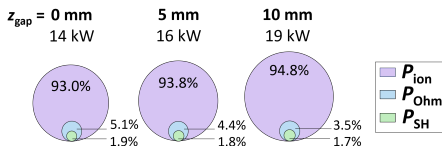
- $P_{\text{Ohm}}/(P_{\text{Ohm}} + P_{\text{SH}})$ versus the magnetic field parameter z_{gap}
- For increasing z_{gap} (lower magnetic field), the fraction $P_{\text{Ohm}}/(P_{\text{Ohm}} + P_{\text{SH}})$ decreases – in line with the increase in pulse power
- $P_{\text{Ohm}}/(P_{\text{Ohm}} + P_{\text{SH}})$ can be regarded as a measure for energy efficiency of a discharge



From Rudolph et al. (2021) JPD submitted for publication



Electron power absorption



From Rudolph et al. (2021) JPD submitted for publication

- The use of the pulse power for different values of z_{gap}
 - ion acceleration (P_{ion})
 - Ohmic heating (P_{Ohm})
 - sheath energization (P_{SH}).
- Most of the pulse power $\langle P_{\text{pulse}} \rangle$ is used to accelerate ions and this power is finally dissipated in the target as heat
- The fraction of the pulse power that is absorbed by the electrons decreases for higher values of z_{gap} and more energy is spent on heating up the target



Deposition rate

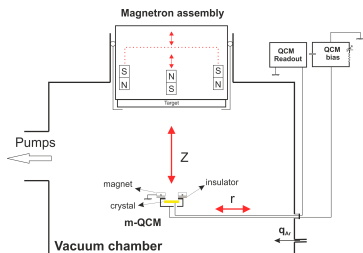


Deposition rate

- The Ti deposition rate and the ionized flux fraction are measured using a gridless ion meter (m-QCM)

Kubart et al. (2014) *SCT* **238** 152

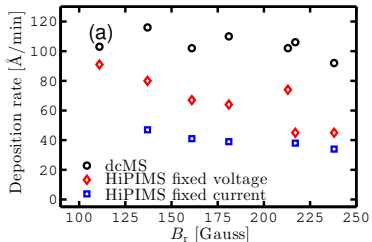
- The ion meter is mounted on a probe holder which can be moved around within the chamber
- The Ar working gas pressure was set to 1 Pa
- In all cases the pulse width was $100 \mu\text{s}$ at an average power of 300 W
- The confining magnetic field is varied by moving the magnets



From Hajihoseini et al. (2019) *Plasma* **2** 201

Deposition rate

- The Ti deposition rate recorded at substrate position using a gridless ion meter (m-QCM)
 - **dcMS**
 - +10% with decreasing $|\mathbf{B}|$ (but no obvious trend)
 - **HiPIMS fixed voltage**
 - +110% with decreasing $|\mathbf{B}|$
 - **HiPIMS fixed peak current**
 - +40% with decreasing $|\mathbf{B}|$
- In HiPIMS operation the deposition rate increases with decreasing $|\mathbf{B}|$



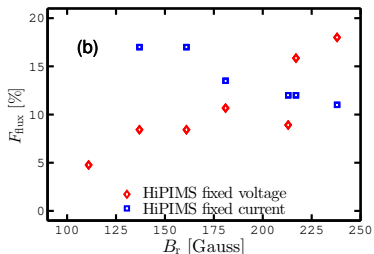
From Gudmundsson (2020) *PSST* **29**(11) 113001

based on Hajihoseini et al. (2019) *Plasma* **2** 201



Deposition rate – Ionized flux fraction

- Ionized flux fraction recorded
 - **dcMS**
Always around 0 %
(Kubart et al., 2014)
 - **HiPIMS fixed voltage**
–75% with decreasing $|\mathbf{B}|$
 - **HiPIMS fixed peak current**
+50% with decreasing $|\mathbf{B}|$
- The ionized flux fraction decreases with decreasing $|\mathbf{B}|$ when the HiPIMS discharge is operated in fixed voltage mode but increases in fixed peak current mode
- Opposing trends



From Gudmundsson (2020) *PSST* **29**(11) 113001

based on Hajihoseini et al. (2019) *Plasma* **2** 201



Deposition rate – α_t and β_t

- Low deposition rate is the main drawback of this sputter technology and hampers its use for industrial applications
- The main reason for the low deposition rate of the HiPIMS discharge is suggested to be due to the back-attraction of the ions of the sputtered species to the cathode target
- Increased deposition rate in HiPIMS often comes at the cost of a lower ionized flux fraction of the sputtered material
- Two internal parameters are of importance
 - α_t – ionization probability
 - β_t – back-attraction probability



Deposition rate – α_t and β_t

- We can relate the measured quantities normalized deposition rate $F_{DR,sput}$ and the ionized flux fraction $F_{ti,flux}$

$$F_{DR,sput} = \frac{\Gamma_{DR}}{\Gamma_0} = (1 - \alpha_t \beta_t)$$

$$F_{ti,flux} = \frac{\Gamma_{DR,ions}}{\Gamma_{DR,sput}} = \frac{\Gamma_0 \alpha_t (1 - \beta_t)}{\Gamma_0 (1 - \alpha_t \beta_t)} = \frac{\alpha_t (1 - \beta_t)}{(1 - \alpha_t \beta_t)}$$

to the internal parameters back attraction probability β_t

$$\beta_t = \frac{1 - F_{DR,sput}}{1 - F_{DR,sput}(1 - F_{ti,flux})}$$

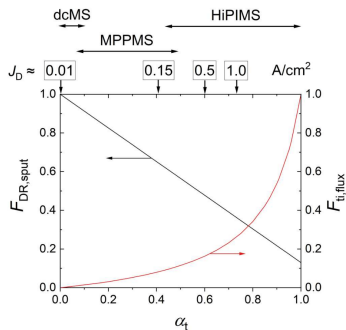
and ionization probability α_t

$$\alpha_t = 1 - F_{DR,sput}(1 - F_{ti,flux})$$



Deposition rate – Optimization

- There are two measures of how good a HiPIMS discharge is:
 - the fraction $F_{DR,sput}$ of all the sputtered material that reaches the diffusion region (DR)
 - the fraction $F_{ti,flux}$ of ionized species in that flux
- There is a trade off between the goals of higher $F_{DR,sput}$ and higher $F_{ti,flux}$
- The figure shows $F_{DR,sput}$ and $F_{ti,flux}$ as functions of α_t at assumed fixed value of $\beta_t = 0.87$

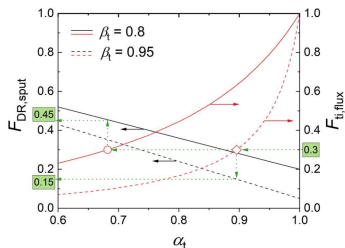


From Brenning et al. (2020) JVSTA 38 033001



Deposition rate – Optimization

- For a particular application an ionized flux fraction of 30 % is suitable but $0.8 \leq \beta_t \leq 0.95$
- If the back-attraction can be reduced to $\beta_t = 0.8$ the deposition rate is increased
- The solid lines show that reducing the back-attraction to $\beta_t = 0.8$ where $\alpha_t = 0.69$ is sufficient to maintain $F_{ti,flux} = 0.30$ (red circle) $F_{DR,sput} = 0.45$ or a factor of three increase in the deposition rate
- The question that remains:
 - How can we vary the ionization probability α_t and maybe more importantly the back-attraction probability β_t ?



From Brenning et al. (2020) *JVSTA* **38** 033008



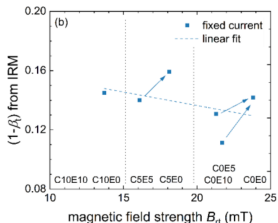
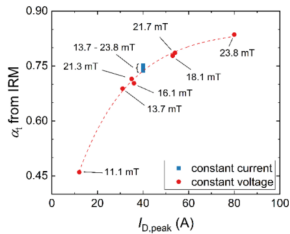
Deposition rate – α_t and β_t

- The internal discharge parameters α_t and β_t from the ionization region model (IRM)

Huo et al. (2017) JPD **50** 354003

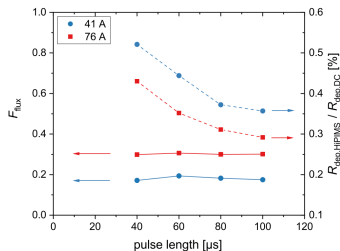
- The ionization probability α_t increases with increased discharge current
- The ion escape fraction $(1 - \beta_t)$ versus the magnetic field strength

From Rudolph et al. (2021a) manuscript in preparation



Deposition rate – Pulse length

- For the same average power, shorter pulses give higher deposition rate than longer pulses
- To maintain the same average power the frequency is varied
- Shortening the pulses does not affect the ionized flux fraction, which remains essentially constant
 - with shorter pulses, the afterglow contributes increasingly more to the total deposition rate
 - the ionized flux fraction from the afterglow is typically higher compared to that during the pulse due to absent back-attracting electric field



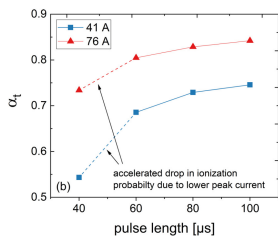
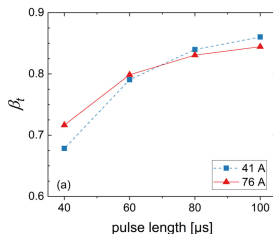
From Rudolph et al. (2020) *PSST* **29** 05LT01



Deposition rate – Pulse length

- By switching-off the cathode potential during the afterglow decreases the effective β_t
- β_t decreases with decreasing pulse length
- The relative contribution of the afterglow ions to the flux toward the DR increases steadily for shorter pulses
- The ionization probability α_t also decreases with a shorter pulse length
- The useful fraction of the sputtered species therefore increases

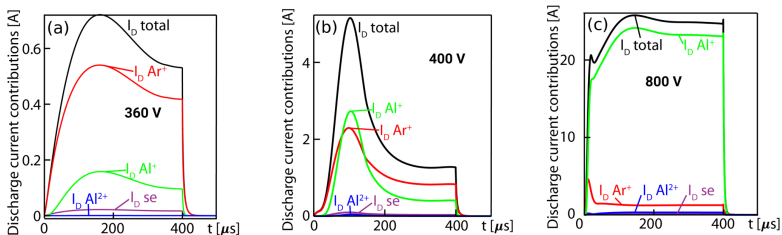
$$F_{\text{DR,sput}} = \frac{\Gamma_{\text{DR}}}{\Gamma_0} = (1 - \alpha_t \beta_t)$$



Recycling in HiPIMS discharges



Recycling in HiPIMS discharges



- A **non-reactive** discharge with 50 mm diameter Al target
- Current composition at the target surface

From Huo et al. (2017) JPD **50** 354003

Experimental data from Anders et al. (2007) JAP **102** 113303



Recycling in HiPIMS discharges

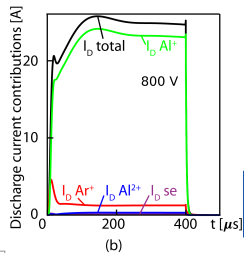
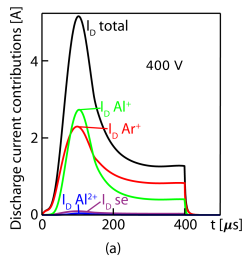
- A primary current I_{prim} is defined as ions of the working gas, here Ar^+ , that are ionized for the first time and then drawn to the target
- This is the dominating current in dc magnetron sputtering discharges
- This current has a critical upper limit

$$I_{\text{crit}} = S_{\text{RT}} e p_{\text{g}} \sqrt{\frac{1}{2\pi m_{\text{g}} k_{\text{B}} T_{\text{g}}}} = S_{\text{RT}} e n_{\text{g}} \sqrt{\frac{k_{\text{B}} T_{\text{g}}}{2\pi m_{\text{g}}}}$$

- Discharge currents I_{D} above I_{crit} are only possible if there is some kind of recycling of atoms that leave the target, become subsequently ionized and then are drawn back to the target

Recycling in HiPIMS discharges

- For the 50 mm diameter Al target the critical current is $I_{crit} \approx 7$ A
- The experiment is operated from far below I_{crit} to high above it, up to 36 A.
- With increasing discharge current I_{prim} gradually becomes a very small fraction of the total discharge current I_D
- The current becomes mainly carried by singly charged Al^+ -ions, meaning that **self-sputter recycling** or the current $I_{SS-recycle}$ dominates



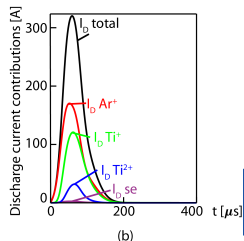
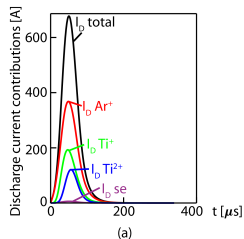
From Huo et al. (2017) JPD **50** 354003

Experimental data from Anders et al. (2007) JAP **102** 113303

Recycling in HiPIMS discharges

- For discharges with Ti target the peak current is far above the critical current (up to 650 A, while $I_{\text{crit}} \approx 19$ A)
- However, this discharge shows close to a 50/50 combination of **self-sputter recycling** $I_{\text{SS-recycle}}$ and **working gas-recycling** $I_{\text{gas-recycle}}$
- Almost 2/3 of the current to the target is here carried by Ar^+ and Ti^{2+} -ions, which both can emit secondary electrons upon target bombardment, and this gives a significant sheath energization

From Huo et al. (2017) JPD **50** 354003



Recycling in HiPIMS discharges

- The total discharge current is

$$I_D = I_{\text{prim}} + I_{\text{gas-recycle}} + I_{\text{SS}}$$

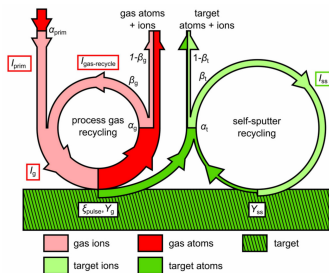
$$= I_{\text{prim}} \left(1 + \frac{\pi_g}{1 - \pi_g} \right) \left(1 + \frac{Y_g}{Y_{\text{SS}}} \frac{\pi_{\text{SS}}}{1 - \pi_{\text{SS}}} \right)$$

where the working gas-sputtering parameter is

$$\pi_g = \alpha_g \beta_g \xi_{\text{pulse}}$$

and the self-sputter parameter

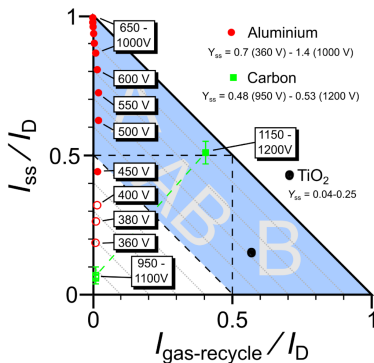
$$\pi_{\text{SS}} = \alpha_t \beta_t Y_{\text{SS}}$$



From Brenning et al. (2017) PSST 26 125003

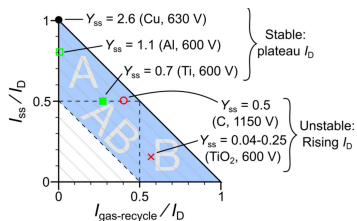
Recycling in HiPIMS discharges

- With increased discharge voltage the discharge with Al target moves from the dcMS regime to the HiPIMS discharge regime – **type A**
- A discharge with carbon target jumps from the dcMS regime to the HiPIMS regime – both SS recycling and working gas recycling play a role – intermediate **type AB**
- For reactive sputtering of Ti target in poisoned mode working gas recycling dominates – **type B**



Recycling in HiPIMS discharges

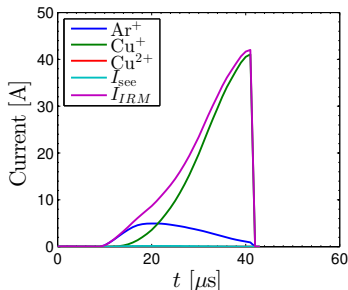
- Recycling map for five different targets with varying self-sputter yield
 - Cu – $Y_{SS} = 2.6$
 - Al – $Y_{SS} = 1.1$
 - Ti – $Y_{SS} = 0.7$
 - C – $Y_{SS} = 0.5$
 - TiO_2 – $Y_{SS} = 0.04 - 0.25$
- For very high self-sputter yields $Y_{SS} > 1$, the discharges above I_{crit} are of **type A** with dominating **SS-recycling**
- For very low self-sputter yields $Y_{SS} < 0.2$, the discharges above I_{crit} are of **type B** with dominating **working gas recycling**



From Brenning et al. (2017) PSST **26** 125003

Recycling in HiPIMS discharges – copper

- The temporal evolution of the discharge current composition at the target surface for a peak discharge current density 2 A/cm^2
- A discharge with 2 inch copper target – $I_{\text{crit}} \approx 3.8 \text{ A}$
- The Cu^+ ion is the dominating positively charged species in the discharge
- The ionized flux fraction of copper is roughly 15 %

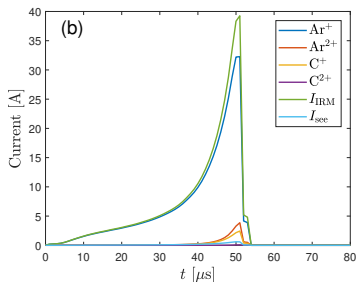


From Gudmundsson et al. (2021) manuscript in preparation



Recycling in HiPIMS discharges – carbon

- The temporal evolution of the discharge current composition at the target surface for a peak discharge current density 2 A/cm^2
- A discharge with 2 inch graphite target – $I_{\text{crit}} \approx 7.6 \text{ A}$
- The Ar^+ ion is the dominating positively charged species in the discharge
- Less than 5 % of the total discharge current is carried by C^+ ions
- The ionized flux fraction of carbon is roughly 2 %

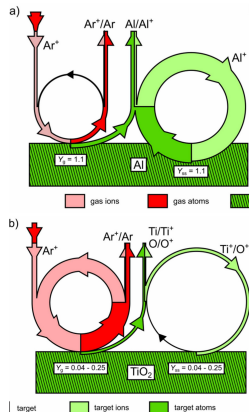


From Eliasson et al. (2021) manuscript in preparation



Recycling in HiPIMS discharges

- Recycling loops
- Discharge with Al or Cu target – SS recycling dominates
 - high self sputter yield
- Reactive discharge with graphite or TiO_2 target – working gas recycling dominates
 - low self sputter yield



Summary



Summary

- Ohmic heating of the electrons can play a significant role in both dc magnetron sputtering discharge and in particular HiPIMS
- There is an inescapable conflict between the goals of higher deposition rate and higher fraction of ionized species in the sputtered material flux
- In HiPIMS discharge operation there is always recycling:
 - For high currents the discharge with Al or Cu target develops almost pure **self-sputter recycling**, while the discharge with Ti target exhibits close to a 50/50 combination of **self-sputter recycling** and **working gas-recycling**
 - For a poisoned Ti, or a graphite target the sputter yield is low and **working gas-recycling** necessary at high currents



Thank you for your attention

- The work is in collaboration with
 - Prof. Daniel Lundin, Linköping University, Sweden
 - Prof. Nils Brenning, KTH Royal Institute of Technology, Stockholm, Sweden
 - Dr. Michael A. Raadu, KTH Royal Institute of Technology, Stockholm, Sweden
 - Dr. Martin Rudolph, Leibniz Institute of Surface Engineering (IOM), Leipzig, Germany
 - Prof. Tiberu Minea, Université Paris-Sud, Orsay, France
 - Dr. Hamidreza Hajihoseini, now at University of Twente, The Netherlands

The slides can be downloaded at

<http://langmuir.raunvis.hi.is/~tumi/ranns.html>

and the project is funded by

- Icelandic Research Fund Grant Nos. 130029 and 196141



References

- Alami, J., P. O. A. Petersson, D. Music, J. T. Gudmundsson, J. Bohlmark, and U. Helmersson (2005). Ion-assisted physical vapor deposition for enhanced film deposition on non-flat surfaces. *Journal of Vacuum Science and Technology A* 23(2), 278–280.
- Anders, A., J. Andersson, and A. Ehasarian (2007). High power impulse magnetron sputtering: Current-voltage-time characteristics indicate the onset of sustained self-sputtering. *Journal of Applied Physics* 102(11), 113303.
- Anders, A., J. Čapek, M. Hála, and L. Martinu (2012). The 'recycling trap': a generalized explanation of discharge runaway in high-power impulse magnetron sputtering. *Journal of Physics D: Applied Physics* 45(1), 012003.
- Brenning, N., A. Butler, H. Hajihoseini, M. Rudolph, M. A. Raadu, J. T. Gudmundsson, T. Minea, and D. Lundin (2020). Optimization of HiPIMS discharges: The selection of pulse power, pulse length, gas pressure, and magnetic field strength. *Journal of Vacuum Science and Technology A* 38(3), 033008.
- Brenning, N., J. T. Gudmundsson, D. Lundin, T. Minea, M. A. Raadu, and U. Helmersson (2016). The role of Ohmic heating in dc magnetron sputtering. *Plasma Sources Science and Technology* 25(6), 065024.
- Brenning, N., J. T. Gudmundsson, M. A. Raadu, T. J. Petty, T. Minea, and D. Lundin (2017). A unified treatment of self-sputtering, process gas recycling, and runaway for high power impulse sputtering magnetrons. *Plasma Sources Science and Technology* 26(12), 125003.
- Depla, D., S. Mahieu, and R. De Gryse (2009). Magnetron sputter deposition: Linking discharge voltage with target properties. *Thin Solid Films* 517(9), 2825–2839.
- Gudmundsson, J. T. (2020). Physics and technology of magnetron sputtering discharges. *Plasma Sources Science and Technology* 29(11), 113001.
- Gudmundsson, J. T. and A. Hecimovic (2017). Foundations of dc plasma sources. *Plasma Sources Science and Technology* 26(12), 123001.
- Gudmundsson, J. T. and D. Lundin (2020). Introduction to magnetron sputtering. In D. Lundin, T. Minea, and J. T. Gudmundsson (Eds.), *High Power Impulse Magnetron Sputtering: Fundamentals, Technologies, Challenges and Applications*, pp. 1–48. Amsterdam, The Netherlands: Elsevier.
- Gudmundsson, J. T., D. Lundin, N. Brenning, M. A. Raadu, C. Huo, and T. M. Minea (2016). An ionization region model of the reactive Ar/O₂ high power impulse magnetron sputtering discharge. *Plasma Sources Science and Technology* 25(6), 065004.

References

- Hajihoseini, H., M. Čada, Z. Hubička, S. Ůnaldi, M. A. Raadu, N. Brenning, J. T. Gudmundsson, and D. Lundin (2019). The effect of magnetic field strength and geometry on the deposition rate and ionized flux fraction in the HiPIMS discharge. *Plasma 2*(2), 201–221.
- Huo, C., D. Lundin, J. T. Gudmundsson, M. A. Raadu, J. W. Bradley, and N. Brenning (2017). Particle-balance models for pulsed sputtering magnetrons. *Journal of Physics D: Applied Physics* 50(35), 354003.
- Huo, C., D. Lundin, M. A. Raadu, A. Anders, J. T. Gudmundsson, and N. Brenning (2014). On the road to self-sputtering in high power impulse magnetron sputtering: particle balance and discharge characteristics. *Plasma Sources Science and Technology* 23(2), 025017.
- Kateb, M., H. Hajihoseini, J. T. Gudmundsson, and S. Ingvarsson (2019). Role of ionization fraction on the surface roughness, density, and interface mixing of the films deposited by thermal evaporation, dc magnetron sputtering, and HiPIMS: An atomistic simulation. *Journal of Vacuum Science and Technology A* 37(3), 031306.
- Kubart, T., M. Čada, D. Lundin, and Z. Hubička (2014). Investigation of ionized metal flux fraction in HiPIMS discharges with Ti and Ni targets. *Surface and Coatings Technology* 238, 152–157.
- Raadu, M. A., I. Axnäs, J. T. Gudmundsson, C. Huo, and N. Brenning (2011). An ionization region model for high power impulse magnetron sputtering discharges. *Plasma Sources Science and Technology* 20(6), 065007.
- Rudolph, M., N. Brenning, H. Hajihoseini, M. A. Raadu, T. M. Minea, A. Anders, D. Lundin, and J. T. Gudmundsson (2021). Influence of the magnetic field on the discharge physics of a high power impulse magnetron sputtering discharge. *Journal of Physics D: Applied Physics*, submitted for publication.
- Rudolph, M., N. Brenning, M. A. Raadu, H. Hajihoseini, J. T. Gudmundsson, A. Anders, and D. Lundin (2020). Optimizing the deposition rate and ionized flux fraction by tuning the pulse length in high power impulse magnetron sputtering. *Plasma Sources Science and Technology* 29(5), 05LT01.
- Rudolph, M., H. Hajihoseini, M. A. Raadu, J. T. Gudmundsson, N. Brenning, T. M. Minea, A. Anders, and D. Lundin (2021). On how to measure the probabilities of target atom ionization and target ion back-attraction in high-power impulse magnetron sputtering. *Journal of Applied Physics* 129(3), 033303.
- Samuelsson, M., D. Lundin, J. Jensen, M. A. Raadu, J. T. Gudmundsson, and U. Helmersson (2010). On the film density using high power impulse magnetron sputtering. *Surface and Coatings Technology* 202(2), 591–596.
- Thornton, J. A. (1978). Magnetron sputtering: basic physics and application to cylindrical magnetrons. *Journal of Vacuum Science and Technology* 15(2), 171–177.